Elastic solution of axisymmetric thick truncated conical shells based on first-order shear deformation theory

M. Ghannad*, M. Zamani Nejad**, G. H. Rahimi***

*Mechanical Engineering Faculty, Shahrood University of Technology, Shahrood, Iran,
E-mail: ghannad.mehdi@gmail.com
**Mechanical Engineering Department, Tarbiat Modares University, Tehran, Iran, E-mail: m.zamani.n@ gmail.com
**Mechanical Engineering Department, Yasouj University, Yasouj P. O. Box: 75914-353, Iran
***Mechanical Engineering Department, Tarbiat Modares University, Tehran, Iran, E-mail: gh.rahimi.s@gmail.com

1. Introduction

Generally, shells are curved structures which exhibit significant stiffness against forces and moments. Scientists have paid an enormous amount of attention to shells, resulting in numerous theories about their behavior. Of different kinds of shells, due to their extensive use in rocket and shuttle cones, conical shells have been of especially importance. Given the limitations of the classic theories of thick wall shells, very little attention has been paid to the analytical solution of these shells.

Naghdi and Cooper [1], assuming the cross shear effect, formulated the theory of shear deformation. Mirsky and Hermann [2], derived the solution of thick cylindrical shells of homogenous and isotropic materials, using the first shear deformation theory. Greenspon [3], opted to make a comparison between the findings regarding the different solutions obtained for cylindrical shells. Making use of Mirsky-Hermann theory and the finite difference method (FDM), Ziv and Perl [4], obtained the vibration response for semilong cylindrical shells. Using the shear deformation theory and Frobenius series, Suzuki et. al. [5], obtained the solution of free vibration of cylindrical shells with variable thickness, and Takashaki et. al. [6], obtained the same solution for conical shells. Applying a three-dimensional (3D) method of analysis, the free vibration frequencies and mode shapes of spherical shell segments with variable thickness are determined [7]. A paper was also published by Kang and Leissa [8] where equations of motion and energy functionals were derived for 3D coordinate system. The field equations are utilized to express them in terms of displacement components . Assuming that the material has a graded modulus of elasticity, while the Poisson's ratio is a constant, Tutuncu and Ozturk [9] investigated the stress distribution in the axisymmetric structures. They obtained the closed-form solutions for stresses and displacements in functionally graded cylindrical and spherical vessels under internal pressure. However, it needs to be pointed out that in deriving and, thus, plotting circumferential stress, Tutuncu & Ozturk made a mistake, which was pointed out by Shi et. al. [10] and Ghannad et. al. [11]. Assuming that a heterogeneous system is composed of the elements with different properties, in the paper [12] the reactions of pipeline systems to shock impact load and the possibilities of the simulation and evaluation of dynamic processes are investigated. Another general analysis of one-dimensional steady-state thermal stresses in a hollow thick cylinder made of functionally graded material (FGM) was obtained [13]. Eipakchi *et. al.*

[14], obtained the solution of the homogenous and isotropic thick-walled cylindrical shells with variable thickness, using the first-order shear deformation theory (FSDT) and the perturbation theory. The stress state of two-layer hollow bars in which they are exposed to axial load is analyzed [15]. The layers are made of isotropic, homogeneous, linearly elastic material, and they are considered as concentric cylinders. Assuming that the material properties vary nonlinearly in the radial direction and the Poisson's ratio is constant, Zamani Nejad and Rahimi [16], obtained closed form solutions for one-dimensional steady-state thermal stresses in a rotating functionally graded pressurized thick-walled hollow circular cylinder. A complete and consistent 3D set of field equations has been developed by tensor analysis to characterize the behavior of FGM thick shells of revolution with arbitrary curvature and variable thickness along the meridional direction [17]. Zamani Nejad and Rahimi [18], obtained stresses in isotropic rotating thick-walled cylindrical pressure vessels made of functionally graded material as a function of radial direction by using the theory of elasticity.

In the present study, the general solution of the thick truncated conical shells will be presented, making use of the FSDT. The governing equations, which are a system of ordinary differential equations with variable coefficients, have been solved analytically using the matched asymptotic method (MAM) of the perturbation theory.

2. Analysis

In the classical theory of shells, the assumption is that the sections that are straight and perpendicular to the mid-plane remain in the same position even after deformation. In the first-order shear deformation theory, the sections that are straight and perpendicular to the mid-plane remain straight but not necessarily perpendicular after deformation and loading. In this case, shear strain and shear stress are taken into consideration.

In Fig. 1, the location of a typical point m, (r), within the shell element may be determined by R and z, as

$$r = R(x) + z \qquad (1)$$

where R represents the distance of middle surface from the axial direction, and z is the distance of typical point from the middle surface.

In Eq. (1), x and z must be within the following ranges

$$0 \le x \le L$$
$$-\frac{h}{2} \le z \le \frac{h}{2} \Bigg\}$$
(2)

where h and L are the thickness and the length of the cone.

$R(x)$ and inner and outer radii (r_i, r_o) of the cone are as follows (Fig. 1)

$$R(x) = a + \frac{h}{2} - (a-b)\frac{x}{L} \Bigg\}$$
$$r_i = R - \frac{h}{2} \ , \ \ r_o = R + \frac{h}{2} \Bigg\}$$
(3)

The general axisymmetric displacement field (U_x, U_z), in the first-order Mirsky-Hermann's theory could be expressed on the basis of axial displacement and radial displacement, as follows

$$U_x = u(x) + \phi(x)z \Big\}$$
$$U_z = w(x) + \psi(x)z \Big\}$$
(4)

where $u(x)$ and $w(x)$ are the displacement components of the middle surface. Also, $\phi(x)$ and $\psi(x)$ are the functions used to determine the displacement field.
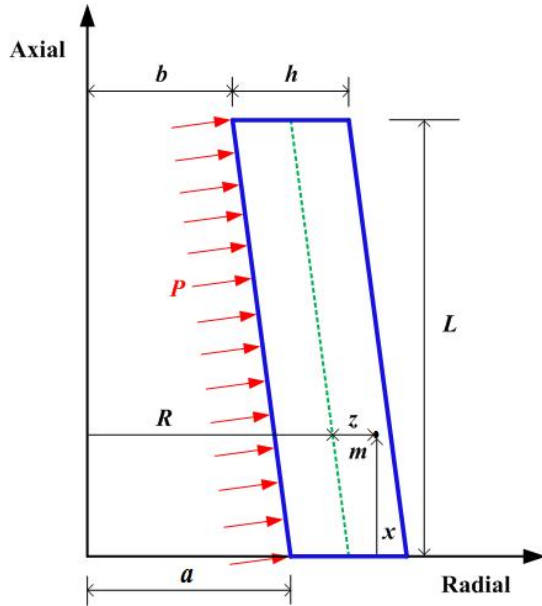

Fig. 1 Geometry of the cone

The strain-displacement relations in the cylindrical coordinates system are

$$\varepsilon_x = \frac{\partial U_x}{\partial x} = \frac{du}{dx} + \frac{d\phi}{dx}z$$
$$\varepsilon_\theta = \frac{U_z}{r} = \frac{w}{R+z} + \frac{\psi}{R+z}z$$
$$\varepsilon_z = \frac{\partial U_z}{\partial z} = \psi$$
$$\gamma_{xz} = \frac{\partial U_x}{\partial z} + \frac{\partial U_z}{\partial x} = \left(\phi + \frac{dw}{dx}\right) + \frac{d\psi}{dx}z$$
(5)

In addition, the stresses on the basis of constitutive equations for homogenous and isotropic materials are as follows

$$\sigma_i = \lambda E\left[(1-\upsilon)\varepsilon_i + \upsilon(\varepsilon_j + \varepsilon_k)\right], \quad i \ne j \ne k$$
$$\tau_{xz} = \frac{\lambda}{2}(1-2\upsilon)E\gamma_{xz}$$
$$\lambda = \frac{1}{(1+\upsilon)(1-2\upsilon)}$$
(6)

where σ_i and ε_i are the stresses and strains in the axial (x), circumferential (θ), and radial (z) directions. υ and E are Poisson's ratio and modulus of elasticity, respectively.

The normal forces (N_x, N_θ, N_z), shear force (Q_x), bending moments (M_x, M_θ), and the torsional moment (M_{xz}) in terms of stress resultants are

$$\begin{Bmatrix} N_x \\ N_\theta \\ N_z \end{Bmatrix} = \int_{-h/2}^{h/2} \begin{Bmatrix} \sigma_x\left(1+\dfrac{z}{R}\right) \\ \sigma_\theta \\ \sigma_z\left(1+\dfrac{z}{R}\right) \end{Bmatrix} dz$$
(7)

$$\begin{Bmatrix} M_x \\ M_\theta \end{Bmatrix} = \int_{-h/2}^{h/2} \begin{Bmatrix} \sigma_x\left(1+\dfrac{z}{R}\right) \\ \sigma_\theta \end{Bmatrix} zdz$$
(8)

$$Q_x = \int_{-h/2}^{h/2} \tau_{xz}\left(1+\frac{z}{R}\right)dz$$
(9)

$$M_{xz} = \int_{-h/2}^{h/2} \tau_{xz}\left(1+\frac{z}{R}\right)zdz$$
(10)

On the basis of the principle of virtual work, the variations of strain energy are equal to the variations of the external work as follows

$$\delta U = \delta W$$
(11)

where U is the total strain energy of the elastic body and W is the total external work due to internal pressure. The strain energy is

$$U = \iiint_V U^* dV \ , \ dV = rdrd\theta dx = (R+z)dzd\theta dx \Bigg\}$$
$$U^* = \frac{1}{2}(\sigma_x\varepsilon_x + \sigma_\theta\varepsilon_\theta + \sigma_z\varepsilon_z + \tau_{xz}\gamma_{xz})$$
(12)

and the external work is

$$W = \iint_S \left(\vec{f}\,\vec{u}\right)dS, \ dS = r_i d\theta dx = \left(R - \frac{h}{2}\right)d\theta dx \Bigg\}$$
$$\vec{f}\,\vec{u} = P_x U_x + P_z U_z$$
(13)

where P_x and P_z are components of internal pressure P along axial and radial directions, respectively.

The variation of the strain energy is

$$\delta U = \int\limits_0^{2\pi}\int\limits_0^L\int\limits_{-h/2}^{h/2} R(x)\delta U^*\left(1+\frac{z}{R}\right)dzdxd\theta \qquad (14)$$

The resulting Eq. (14) will be

$$\frac{\delta U}{2\pi} = \int\limits_0^L R(x)\int\limits_{-h/2}^{h/2}\left(\sigma_x\delta\varepsilon_x + \sigma_\theta\delta\varepsilon_\theta + \right.$$
$$\left. +\sigma_z\delta\varepsilon_z + \tau_{xz}\delta\gamma_{xz}\right)\left(1+\frac{z}{R}\right)dzdx \qquad (15)$$

and the variation of the external work is

$$\delta W = \int\limits_0^{2\pi}\int\limits_0^L\left(P_x\delta U_x + P_z\delta U_z\right)\left(R-\frac{h}{2}\right)dxd\theta \qquad (16)$$

The resulting Eq. (16) will be

$$\frac{\delta W}{2\pi} = \int\limits_0^L\left(P_x\delta U_x + P_z\delta U_z\right)\left(R-\frac{h}{2}\right)dx \qquad (17)$$

Substituting Eqs. (5) and (6) into Eqs. (15) and (17), and drawing upon calculus of variation and the virtual work principle, we will have

$$\left.\begin{array}{l}\dfrac{d}{dx}\left(RN_x\right) = -P_x\left(R-\dfrac{h}{2}\right) \\[2mm] \dfrac{d}{dx}\left(RM_x\right) - RQ_x = P_x\dfrac{h}{2}\left(R-\dfrac{h}{2}\right) \\[2mm] \dfrac{d}{dx}\left(RQ_x\right) - N_\theta = -P_z\left(R-\dfrac{h}{2}\right) \\[2mm] \dfrac{d}{dx}\left(RM_{xz}\right) - M_\theta - RN_z = P_z\dfrac{h}{2}\left(R-\dfrac{h}{2}\right)\end{array}\right\} \qquad (18)$$

And the boundary conditions are

$$\left[R\left(N_x\delta u + M_x\delta\phi + Q_x\delta w + M_{xz}\delta\psi\right)\right]_0^L = 0 \qquad (19)$$

Eq. (19) states the boundary conditions which must exist at the two ends of the cone.

In order to solve the set of differential Eqs. (18), forces and moments need to be expressed in terms of the components of displacement field, using Eqs. (5) to (10).

In Eqs. (18), it is apparent that u does not exist, but du/dx does. In the set of Eqs. (5), du/dx is needed to calculate displacements. Taking du/dx as v, and integrating the first equations in the set of Eqs. (18)

$$RN_x = -\int P_x\left(R-\frac{h}{2}\right)dx + C_0 \qquad (20)$$

Thus, set of differential Eqs. (18) could be derived as follows

$$\left.\begin{array}{l}\dfrac{d}{dx}\left(\left[A_1\right]\dfrac{d}{dx}\{y\}\right) + \dfrac{d}{dx}\left(\left[A_2\right]\{y\}\right) + \\[2mm] +\left[A_3\right]\dfrac{d}{dx}\{y\} + \left[A_4\right]\{y\} = \{F\} \\[2mm] \{y\} = \{v(x) \quad \phi(x) \quad w(x) \quad \psi(x)\}^T\end{array}\right\} \qquad (21)$$

The set of Eqs. (21) is a set of linear non-homogenous equations with variable coefficients. The general method for solving these equations is the Frobenius method, which requires approximating displacements in terms of power series which are functions of x, substituting in the respective equations and applying boundary conditions in order to calculate the constants.

It is usually the case that the convergence of these series involves numerous terms. For instance, in paper [5], 50 terms and in paper [6], 100 terms are considered. In the present paper, MAM of the perturbation theory has been used to solve these equations.

3. Analytical solution for homogeneous truncated conical shell

We assume that Young's modulus and the Poisson's ratio are constant.

In order to calculate the matrices $\left[A_i\right]_{4\times4}$ in the set of Eq. (21), the stress resultants, obtained in terms of displacement field, are substituted in Eqs. (7) to (10), and integrated.

Thus, forces and moments are obtained as follows

$$\left.\begin{array}{l}N_x = \lambda Eh\left[(1-\upsilon)\left(\dfrac{du}{dx}+\dfrac{h^2}{12R}\dfrac{d\phi}{dx}\right)+\right. \\[2mm] \left.+\upsilon\left(\dfrac{w}{R}+\psi\right)\right] \\[2mm] N_\theta = \lambda Eh\left[\upsilon\dfrac{du}{dx}+\dfrac{(1-\upsilon)\alpha w}{h}+\right. \\[2mm] \left.+\left(1-\dfrac{(1-\upsilon)R\alpha}{h}\right)\psi\right] \\[2mm] N_z = \lambda Eh\left[\upsilon\left(\dfrac{du}{dx}+\dfrac{h^2}{12R}\dfrac{d\phi}{dx}\right)+\right. \\[2mm] \left.+\upsilon\dfrac{w}{R}+(1-\upsilon)\psi\right]\end{array}\right\} \qquad (22)$$

$$\left.\begin{array}{l}M_x = \lambda E\dfrac{h^3}{12R}\left[(1-\upsilon)\left(\dfrac{du}{dx}+R\dfrac{d\phi}{dx}\right)+2\upsilon\psi\right] \\[2mm] M_\theta = \lambda E\dfrac{h^3}{12}\left[\dfrac{12}{h^3}(1-\upsilon)(h-R\alpha)(w-R\psi)+\right. \\[2mm] \left.+\upsilon\dfrac{d\phi}{dx}\right]\end{array}\right\} \qquad (23)$$

$$Q_x = K\frac{(1-2\upsilon)}{2}\lambda Eh\left[\phi+\frac{dw}{dx}+\frac{h^2}{12R}\frac{d\psi}{dx}\right] \qquad (24)$$

$$M_{xz} = K\frac{(1-2\upsilon)}{2}\lambda E\frac{h^3}{12R}\left[\phi+\frac{dw}{dx}+R\frac{d\psi}{dx}\right] \qquad (25)$$

where K is the shear correction factor that is embedded in the shear stress term. It is assumed that in the static state, for conical shells $K = 5/6$ [19]. The parameters μ and α are as follows

$$\mu = K\frac{(1-\upsilon)}{2}, \quad \alpha = ln\left(\frac{R+\dfrac{h}{2}}{R-\dfrac{h}{2}}\right) \qquad (26)$$

The coefficients matrices $\left[A_i\right]_{4\times4}$, and force vector $\{F\}$ are obtained by substituting Eqs. (22) to (25) into Eqs. (18)

$$[A_1] = \begin{bmatrix} 0 & 0 & 0 & 0 \\ 0 & (1-\upsilon)\dfrac{Rh^3}{12} & 0 & 0 \\ 0 & 0 & \mu Rh & \mu\dfrac{h^3}{12} \\ 0 & 0 & \mu\dfrac{h^3}{12} & \mu\dfrac{Rh^3}{12} \end{bmatrix} \qquad (27)$$

$$[A_2] = \begin{bmatrix} 0 & 0 & 0 & 0 \\ (1-\upsilon)\dfrac{h^3}{12} & 0 & 0 & \upsilon\dfrac{h^3}{6} \\ 0 & \mu Rh & 0 & 0 \\ 0 & \mu\dfrac{h^3}{12} & 0 & 0 \end{bmatrix} \qquad (28)$$

$$[A_3] = \begin{bmatrix} 0 & (1-\upsilon)\dfrac{h^3}{12} & 0 & 0 \\ 0 & 0 & -\mu Rh & -\mu\dfrac{h^3}{12} \\ 0 & 0 & 0 & 0 \\ 0 & -\upsilon\dfrac{h^3}{6} & 0 & 0 \end{bmatrix} \qquad (29)$$

$$[A_4] = \begin{bmatrix} (1-\upsilon)Rh & 0 \\ 0 & -\mu Rh \\ -\upsilon h & 0 \\ -\upsilon Rh & 0 \\ \upsilon h & \upsilon Rh \\ 0 & 0 \\ -(1-\upsilon)\alpha & -h+(1-\upsilon)R\alpha \\ -h+(1-\upsilon)R\alpha & -(1-\upsilon)R^2\alpha \end{bmatrix} \qquad (30)$$

$$\{F\} = \frac{1}{\lambda E}\begin{Bmatrix} -\int P_x\left(R-\dfrac{h}{2}\right)dx + C_0 \\ P_x\dfrac{h}{2}\left(R-\dfrac{h}{2}\right) \\ -P_z\left(R-\dfrac{h}{2}\right) \\ P_z\dfrac{h}{2}\left(R-\dfrac{h}{2}\right) \end{Bmatrix} \qquad (31)$$

Given that the set of differential equations (21) do not have exact solutions, for the purpose of solving, MAM of the perturbation theory has been used, in which the convergence of solution is fast.

Solving the equations with variable coefficients gives rise to solving a system of algebraic equations and two systems of differential equations with constant coefficients. These systems of equations have the closed forms solutions. To accomplish this, making use of the characteristic scales, the governing equations are made dimensionless

$$\left.\begin{aligned} x^* &= \frac{x}{L}, & z^* &= \frac{z}{h} \\ h^* &= \frac{h}{h}=1, & R^* &= \frac{R}{h} \\ u^* &= \frac{u}{h}, & w^* &= \frac{w}{h} \end{aligned}\right\} \qquad (32)$$

Substituting dimensionless parameters the set of Eqs. (21) is

$$\left.\begin{aligned} &\varepsilon^2\frac{d}{dx^*}\left([A_1^*]\frac{d}{dx^*}\{y^*\}\right)+\varepsilon\left[\frac{d}{dx^*}\left([A_2^*]\{y^*\}\right)+\right. \\ &\left.+[A_3^*]\frac{d}{dx^*}\{y^*\}\right]+[A_4^*]\{y^*\}=\{F^*\} \\ &\{y^*\}=\{\upsilon \ \ \phi \ \ w^* \ \ \psi\}^T \end{aligned}\right\} \qquad (33)$$

where

$$v = \frac{du}{dx} = \varepsilon\frac{du^*}{dx^*} \qquad (34)$$

Hence,

$$u^* = \frac{1}{\varepsilon}\left[\int v dx^* + C^*\right] \qquad (35)$$

The coefficients matrices $\left[A_i^*\right]_{4\times4}$, and force vector $\{F^*\}$ are obtained as follows

$$[A_1^*] = \begin{bmatrix} 0 & 0 & 0 & 0 \\ 0 & \dfrac{(1-\upsilon)R^*}{12} & 0 & 0 \\ 0 & 0 & \mu R^* & \dfrac{\mu}{12} \\ 0 & 0 & \dfrac{\mu}{12} & \dfrac{\mu R^*}{12} \end{bmatrix} \qquad (36)$$

$$[A_2^*] = \begin{bmatrix} 0 & 0 & 0 & 0 \\ \dfrac{(1-\upsilon)}{12} & 0 & 0 & \dfrac{\upsilon}{6} \\ 0 & \mu R^* & 0 & 0 \\ 0 & \dfrac{\mu}{12} & 0 & 0 \end{bmatrix} \qquad (37)$$

$$\left[A_3^* \right] = \begin{bmatrix} 0 & \dfrac{(1-\upsilon)}{12} & 0 & 0 \\[2mm] 0 & 0 & -\mu R^* & -\dfrac{\mu}{12} \\[2mm] 0 & 0 & 0 & 0 \\[2mm] 0 & -\dfrac{\upsilon}{6} & 0 & 0 \end{bmatrix} \tag{38}$$

$$\left[A_4^* \right] = \begin{bmatrix} (1-\upsilon)R^* & 0 \\ 0 & -\mu R^* \\ -\upsilon & 0 \\ -\upsilon R^* & 0 \\ \upsilon & \upsilon R^* \\ 0 & 0 \\ -(1-\upsilon)\alpha & -1+(1-\upsilon)R^*\alpha \\ -1+(1-\upsilon)R^*\alpha & -(1-\upsilon)R^{*2}\alpha \end{bmatrix} \tag{39}$$

$$\{F^*\} = \frac{1}{\lambda E} \begin{Bmatrix} -\dfrac{P_x}{\varepsilon}\int\left(R^*-\dfrac{1}{2}\right)dx^* + C_0^* \\[3mm] \dfrac{P_x}{2}\left(R^*-\dfrac{1}{2}\right) \\[3mm] -P_z\left(R^*-\dfrac{1}{2}\right) \\[3mm] \dfrac{P_z}{2}\left(R^*-\dfrac{1}{2}\right) \end{Bmatrix} \tag{40}$$

where the parameters are as follows

$$\mu = K\frac{(1-2\upsilon)}{2} \quad, \quad C_0^* = \frac{C_0}{h^2}$$
$$\alpha = ln\left(\frac{R+\dfrac{h}{2}}{R-\dfrac{h}{2}}\right) = ln\left(\frac{R^*+\dfrac{1}{2}}{R^*-\dfrac{1}{2}}\right) \tag{41}$$

The set of Eqs. (33) is singular. Therefore, its solution must be considered in the area of boundary layer problems. For the purpose of solving, MAM of the perturbation theory has been used. As boundary conditions are clamped-clamped, one lies in $x^* = 0$ and the other in $x^* = 1$. So, the solution of the problem contains an outer solution away from the boundaries and two inner solutions near the two boundaries $x^* = 0$ and $x^* = 1$ [20].

4. Results and discussion

The analytical solution described in the preceding section for a homogeneous and isotropic truncated conical shell with $a = 40$ mm, $b = 30$ mm, $h = 20$ mm and $L = 400$ mm will be considered. The Young's Modulus and Poisson's ratio, respectively, have values of $E = 200$ GPa and $\upsilon = 0.3$. The applied internal pressure is 80 MPa. The truncated cone has clamped-clamped boundary conditions.

Fig. 2 shows the distribution of axial displacement at different layers. At points away from the bounda-

ries, axial displacement does not show significant differences in different layers, while at points near the boundaries, the reverse holds true. The distribution of radial displacement at different layers is plotted in Fig. 3. The radial displacement at points away from the boundaries depends on radius and length. According to Figs. 2 and 3, the change in axial and radial displacements in the lower boundary is greater than that of the upper boundary and the greatest axial and radial displacement occurs in the internal surface $(z = -h/2)$. Distribution of circumferential stress in different layers is shown in Fig. 4. The circumferential stress at all points depends on radius and length. The circumferential stress at layers close to the external surface is negative, and at other layers positive. The greatest circumferential stress occurs in the internal surface $(z = -h/2)$.
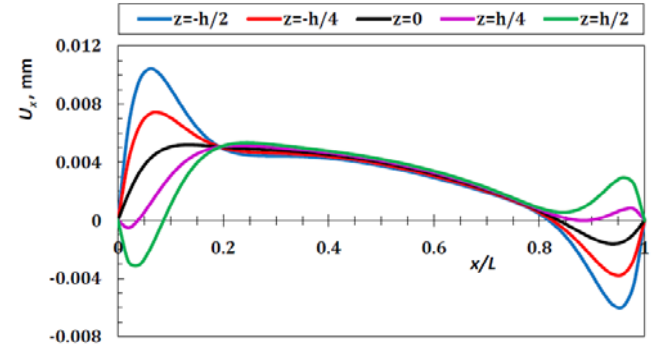

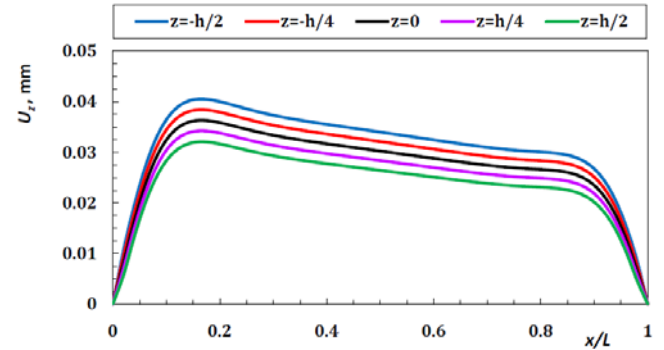Fig. 2 Axial displacement distribution in different layers

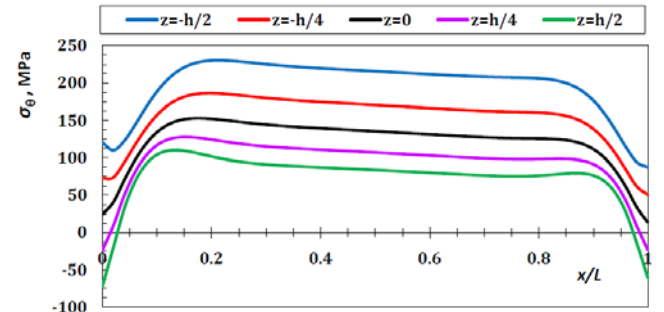Fig. 3 Radial displacement distribution in different layers

Fig. 4 Circumferential stress distribution in different layers

Fig. 5 shows the distribution of shear stress at different layers. The shear stress at points away from the boundaries at different layers is the same and trivial. However, at points near the boundaries, the stress is significant, especially in the internal surface, which is the greatest.

In Figs. 6-9, the effects of the changes in tapering

angles with different values of *a* on axial displacement, radial displacement, circumferential stress, and shear stress will be considered.
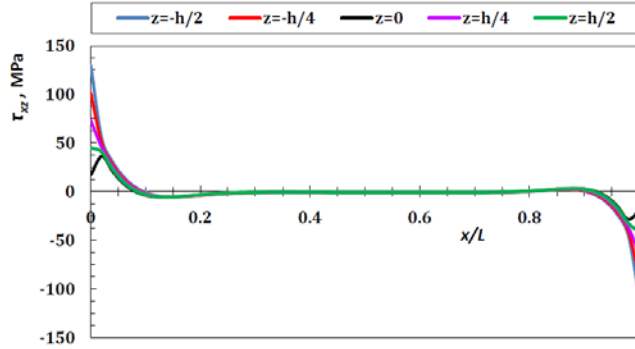

Fig. 5 Shear stress distribution in different layers

The distribution of axial displacement in the inner surface of the cone is shown in Fig. 6. The greater the tapering angle, the greater the displacement, which is significant. In cones with small tapering angles, the greatest axial displacement occurs in the lower boundary. The larger the tapering angles, the greater the axial displacement in the lower boundary and in the middle surface of the cone. The changes in the middle surface are the greatest.
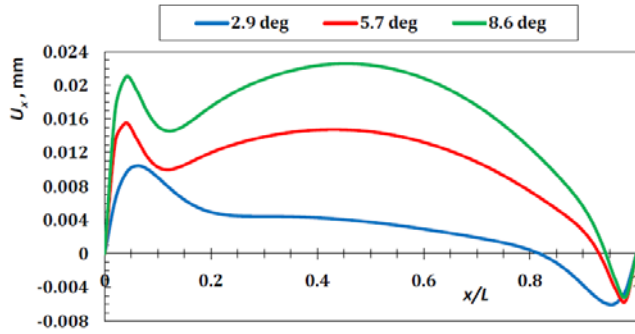

Fig. 6 Axial displacement distribution along inner surface with different tapering angles
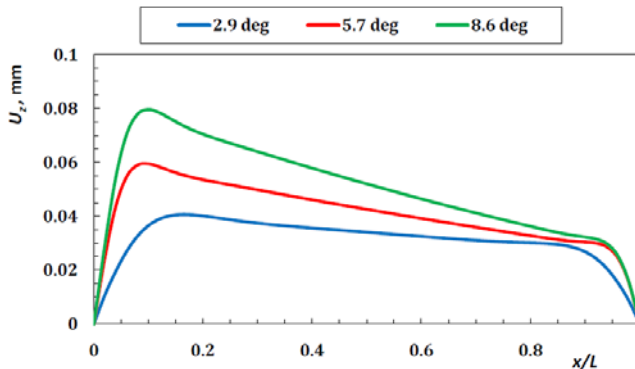

Fig. 7 Radial displacement distribution along inner surface with different tapering angles

The distribution of radial displacement in the inner surface of the cone is shown in Fig. 7. The greater the tapering angle, the greater the radial displacement. The greatest radial displacement occurs in the lower boundary. In cones with small tapering angles, the greatest axial displacement occurs in the lower boundary. The larger tapering angles, the greater the axial displacement in the lower boundary and in the middle surface of the cone. The

changes in the middle surface are the greatest. In a like manner, the distribution of the circumferential stress in the inner surface is illustrated in Fig. 8. As this figure suggests, the greater the tapering angle, the greater the circumferential stress. The distribution of shear stress is shown in Fig. 9. According to this figure, the shear stress at points away from the boundaries is insignificant, and at boundary layers the changes in tapering angles do not have a significant bearing on the shear stress.
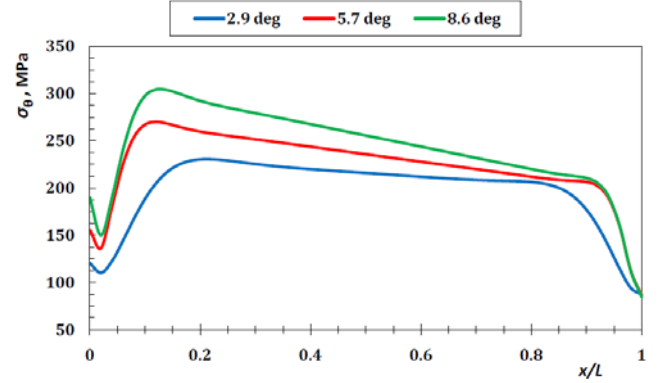

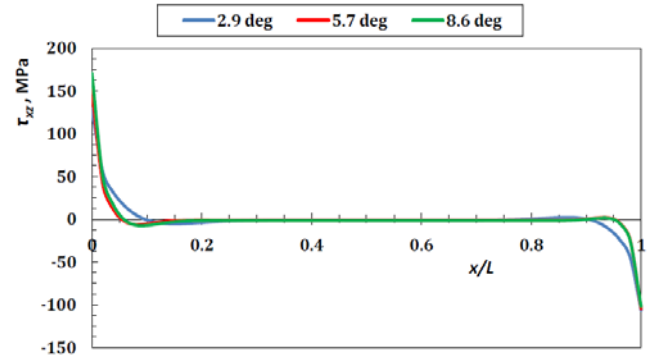Fig. 8 Circumferential stress distribution along inner surface with different tapering angles

Fig. 9 Shear stress distribution along inner surface with different tapering angles

5. Conclusions

In this study, the analytical solution of a thick homogenous and isotropic conical shell is presented, making use of the FSDT. In line with the energy principle and the FSDT, the equilibrium equations have been derived. Using the MAM of the perturbation theory, the system of differential equations which are ordinary and have variable coefficients has been solved analytically. The axial displacement in thick conical shells at points away from the boundaries depends more on the length rather than the radius, whereas at boundaries, this depends on both length and radius. The radial displacement at all points in a conical shell depends on the radius and the length. The circumferential stress at different layers depends on the radius and the length. These changes are relatively great. The greatest values of stress and displacement belong to the inner surface. The shear stress at points away from the boundaries is insignificant, and at boundary layers it is the opposite. The axial displacement, radial displacement, and circumferential stress are heavily dependent on tapering angles and any change in the tapering angle brings about a change in them. However, the shear stress does not undergo similar

changes with changes in tapering angles.

References

1. **Naghdi, P.M., Cooper, R.M.** Propagation of elastic waves in cylindrical shells, including the effects of transverse shear and rotary inertia. -J. of the Acoustical Society of America, 1956, v.29, No1, p.56-63.
2. **Mirsky, I., Hermann, G.** Axially motions of thick cylindrical shells. -J. of Applied Mechanics-Transactions of the ASME, 1958, v.25, p.97-102.
3. **Greenspon, J.E.** Vibration of a thick-walled cylindrical shell, comparison of the exact theory with approximate theories. -J. of the Acoustical Society of America, 1960, v.32, No.5, p.571-578.
4. **Ziv, M., Perl, M.** Impulsive deformation of Mirsky-Hermann's thick cylindrical shells by a numerical method, -J. of Applied Mechanics-Transactions of the ASME, 1973, v.40, No.4, p.1009-1016.
5. **Suzuki, K., Konnon, M., Takahashi, S.** Axisymmetric vibration of a cylindrical shell with variable thickness, -Bulletin of the JSME-Japan Society of Mechanical Engineers, 1981, v.24, No.198, p.2122-2132.
6. **Takahashi, S., Suzuki, K., Kosawada, T.** Vibrations of conical shells with variable thickness, -Bulletin of the JSME-Japan Society of Mechanical Engineers, 1986, v.29, No.285, p.4306-4311.
7. **Kang, J.H., Leissa, A.W.** Three-dimensional vibrations of thick spherical shell segment with variable thickness, -Int. J. of Solids and Structures, 2000, v.37, No.35, p.4811-4823.
8. **Kang, J.H., Leissa, A.W.** Three-dimensional field equations of motion and energy functionals for thick shells of revolution with arbitrary curvature and variable thickness, -J. of Applied Mechanics-Transactions of the ASME, 2001, v.68, No.6, p.953-954.
9. **Tutuncu, N., Ozturk, M.** Exact solution for stresses in functionally graded pressure vessels, Composites: Part B, 2001 v.32, No.8, p.683-686.
10. **Shi, Z.F., Zhang, T.T., Xiang, H.J.** Exact solutions of heterogeneous elastic hollow cylinders, -Composite Structures, 2007, v.79, No.1, p.140-147.
11. **Ghannad, M., Rahimi, G.H., Khadem, S.E.** General shear deformation solution of axisymmetric functionally graded thick cylindrical shells. -J. of Modares Technology and Engineering, 2009, Accepted. (in Press).
12. **Dorosevas, V., Volkovas, V.** Analysis the interaction of two cylindrical surfaces under shock impact load. -Mechanika. -Kaunas: Technologija, 2007, Nr.6(68), p.49-52.
13. **Jabbari, M., Sohrabpour, S., Eslami, M.R.** Mechanical and thermal stresses in a functionally graded hollow cylinder due to radially symmetric loads. -Int. J. of Pressure Vessels and Piping, 2002, v.79, No.7, p.493-497.
14. **Eipakchi, H.R., Rahimi, G.H., Khadem, S.E.** Closed form solution for displacements of thick cylinders with varying thickness subjected to nonuniform internal pressure. -Structural Engineering and Mechanics, 2003, v.16, No.6, p.731-748.
15. **Partaukas, N., Bareisis, J.** The stress state in two-layer hollow cylindrical bars. -Mechanika. -Kaunas: Technologija, 2009, Nr.1(75), p.5-12.
16. **Zamani Nejad, M., Rahimi, G.H.** Deformations and stresses in rotating FGM pressurized thick hollow cylinder under thermal load. -Scientific Research and Essays, 2009, v.4, No3, p.131-140.
17. **Zamani Nejad, M., Rahimi, G.H., Ghannad, M.** Set of field equations for thick shell of revolution made of functionally graded materials in curvilinear coordinate system, -Mechanika. -Kaunas: Technologija, 2009, Nr.3(77), p.18-26.
18. **Zamani Nejad, M., Rahimi, G.H.** Elastic analysis of FGM rotating cylindrical pressure vessels. - Journal of the Chinese Institute of Engineers, 2010, v.33, No4, p.xx-xx. Article in Press.
19. **Vlachoutsis, S.** Shear correction factors for plates and shells, -Int. J. for Numerical Method in Engineering, 1992, v.33, No7, p.1537-1552.
20. **Nayfeh, A.H.** Introduction to Perturbation Techniques. -New York: John Wiley, 1993.-265p.

M. Ghannad, M. Zamani Nejad, G. H. Rahimi

TAMPRIŲ STORŲ ASIMETRINIŲ NUPJAUTOS KŪGINĖS FORMOS KEVALINIŲ STRUKTŪRŲ ANALIZĖ TAIKANT PIRMOS EILĖS ŠLYTIES DEFORMACIJOS TEORIJĄ

R e z i u m ė

Šiame straipsnyje, remiantis pirmos eilės šlyties deformacijos teorija (FSDT) bei virtualaus darbo principu, sudarytos diferencialinės lygtys, išreiškiančios asimetrinius nupjautus kūginės formos storus kevalus. Matematinis modelis išreiškiamas įprasta diferencialinių lygčių su kintamaisiais koeficientais sistema. Taikant sužadinimo (perturbacijos) teorijos suderintąjį asimptočių metodą (MAM), šios lygtys gali būti transformuojamos į algebrinių lygčių sistemą ir dvi diferencialinių lygčių sistemas su pastoviais koeficientais. Sudaryta nauja lygčių sistema turi glaustos formos sprendinį. Ji tinkama esant skirtingam kevalo kūgiškumui, poslinkiams ir įtempiams spinduline ir išilgine kryptimi.

M. Ghannad, M. Zamani Nejad, G. H. Rahimi

ELASTIC SOLUTION OF AXISYMMETRIC THICK TRUNCATED CONICAL SHELLS BASED ON FIRST-ORDER SHEAR DEFORMATION THEORY

S u m m a r y

In this paper, based on first-order shear deformation theory (FSDT), and the virtual work principle, the differential equations governing axisymmetric thick truncated conical shells have been derived. The governing equations are a system of ordinary differential equations with variable coefficients. Using the matched asymptotic method (MAM) of the perturbation theory, these equations could be converted into a system of algebraic equations and two systems of differential equations with constant coefficients. The derived systems of equations have closed form solutions. For different conical angles, displacements and stresses along the radius and length have been plotted.

М. Ганнад, М. Замани Неяд, Г. Н. Рагими

УПРУГОЕ РЕШЕНИЕ АСИММЕТРИЧНЫХ
УСЕЧЕННЫХ ТОЛСТЫХ ОБОЛОЧЕК
КОНИЧЕСКОЙ ФОРМЫ ПРИМЕНЯЯ ТЕОРИЮ
СДВИГА ПЕРВОГО ПОРЯДКА

Р е з ю м е

    В статье, основываясь на теорию сдвига пер-
вого порядка (FSDT) и принцип виртуальной работы
составлены дифференциальные уравнения, описы-
вающие асимметричные усеченные толстые оболочки
конической формы. Математическая модель составле-
на при помощи системы дифференциальных уравне-
ний с переменными коэффициентами. Используя со-
гласованный асимптотический метод (МАМ) из теории
возбуждения (пертурбации), система уравнений
трансформирована в систему алгебраических и диффе-
ренциальных уравнений с переменными коэффициен-
тами. Новая система уравнений сжатой формы подхо-
дит для оболочек разной конусности, для определения
сдвигов, перемещений и напряжений, возникающих в
радиальном и осевом направлениях.